Superconductivity in Geometrically Frustrated Pyrochlore RbOs$_2$O$_6$

M. Brühwiler,* S.M. Kazakov, N.D. Zhigadlo, J. Karpinski, and B. Batlogg

Laboratory for Solid State Physics, ETH Zürich, 8093 Zürich, Switzerland.

(Dated: February 2, 2008)

Abstract

We report the basic thermodynamic properties of the new geometrically frustrated β-pyrochlore bulk superconductor RbOs$_2$O$_6$ with a critical temperature $T_c = 6.4$ K. Specific heat measurements are performed in magnetic fields up to 12 T. The electronic density of states at the Fermi level in the normal state results in $\gamma = (33.7 \pm 0.2)$ mJ/mol$_{f.u.}$/K^2. In the superconducting state, the specific heat follows conventional BCS-type behavior down to 1 K, i.e. over three orders of magnitude in specific heat data. The upper critical field slope at T_c is 1.2 T/K, corresponding to a Maki-parameter $\alpha = 0.64 \pm 0.1$. From the upper critical field $\mu_0 H_{c2} \approx 6$ T at 0 K, we estimate a Ginzburg-Landau coherence length $\xi \approx 74$ Å. RbOs$_2$O$_6$ is the second reported metallic AB$_2$O$_6$ type pyrochlore compound after KOs$_2$O$_6$, and one of only three pyrochlore superconductors in addition to Cd$_2$Re$_2$O$_7$ and KOs$_2$O$_6$.

PACS numbers: 74.25.Op, 74.25.Bt, 74.25.-q, 74.62.-c, 74.70.Dd

---

*Electronic address: bruehwiler@solid.phys.ethz.ch

Nonconducting magnetic compounds with d electrons on a 3-dimensional triangular lattice have been intensely studied. One of the magnetic ground states evolving out of the geometrically frustrated magnet is "spin ice" [1]. Naturally, the question arises if and how itinerant electrons are affected by such a frustrated lattice and what ground state is realized in such systems. The pyrochlores constitute ideal systems for such a study, since the network of the relevant metal atoms consists of corner-sharing tetrahedra. Their electrical properties vary from highly insulating to semiconducting to metallic, the pyrochlores containing 5d transition metal ions being bad metals in general [2]. Surprisingly, superconductivity has been reported for the first time in a pyrochlore for $Cd_2Re_2O_7$ [3, 4, 5], and recently also in KOs_2O_6 [6], and $RbOs_2O_6$ [7]. Aside from the critical temperature, no physical properties of $RbOs_2O_6$ have yet been reported. Here we report thermodynamic measurements on this compound.

The pyrochlore structure in general is of type $A_2B_2O_6O'$, sometimes written as $A_2B_2O_7$, with space-group $F\,d\,\bar{3}\,m$ [2]. The four crystallographically inequivalent atoms in the face-centered cubic unit cell A, B, O, and O', occupy the 16d, 16c, 48f, and 8b sites respectively. The compounds where A is a trivalent and B a tetravalent cation (A^{3+},B^{4+}), and also the (A^{2+},B^{5+}) combination, have been widely studied by various workers. In the β-pyrochlore $RbOs_2O_6$, A is the monovalent cation Rb, and B is the transition metal cation Os octahedrally coordinated by O. It is derived from the parent compound by replacing the O' atoms by Rb atoms and leaving the 16d site empty ($AB_2O_6 \equiv \square_2B_2O_6A'$, where $\square$ represents a vacancy). The Os atoms are coordinated by 6 O atoms and these OsO_6 octahedra share corners. They have edge-lengths of 2.67 and 2.72 Å respectively, and the Os - O bonding distance is 1.91 Å. The electron donating Rb atoms are coordinated by O with a Rb - O distance of 3.13 Å. From X-ray measurements, we refine the 48f oxygen x parameter to 0.315(1). This results in O - Os - O angles in the octahedra of 88.85 ° and 91.15 °.

The B site may accommodate an ion carrying a localized magnetic moment, which interacts antiferromagnetically with its nearest neighbors. Since the B sublattice consists of interconnected tetrahedra, we have to account for the 3-dimensional geometrical frustration of the magnetic interactions, possibly leading to an unconventional groundstate. The inset of Fig. 1 shows an Os atom and its relationship to its surrounding. Every Os atom forms the shared corner of two Os tetrahedra in a network. The exchange pathways to the nearest neighbors, leading by one of the coordinating oxygen atoms, are shown by dashed lines. The

pathways form an Os - O - Os angle of $139.4°$, the direct distance between the two Os being $3.58 \,Å$. The Rb cations are omited in this illustration for clarity. To our knowledge, the B - O - B angle in $RbOs_2O_6$ is surpassed only by one other pyrochlore, the bulk superconductor $Cd_2Re_2O_7$. Together with the high density of states at the Fermi level in this compound, we expect the large B - O - B angle to play a crucial role in the tendency to superconduct. It would therefore be interesting to know how it compares to the corresponding angle in KOs_2O_6.

Formally, the oxidation state of the osmium ion is either $5.5+$ as in $Rb^+Os_2^{5.5+}O_6^{2-}$ or $50\,\%$ $5+$ and $50\,\%$ $6+$ as in $Rb^+Os^{5+}Os^{6+}O_6^{2-}$. Since the ground state configuration of osmium is $[Xe]4f^{14}5d^66s^2$, one would expect the Os^{5+} to be in a spin $S = 3/2$ state, while Os^{6+} is in a spin $S = 1$ state. Band structure calculations for $Cd_2(Os,Re)_2O_7$ [8], show that the crystal field well separates the 5d e_g and t_{2g} bands from each other. The 5d manifold is also well separated from the O 2p band. Although the Os 16c site has trigonal symmetry, this part of the crystal field is weak and there is no further splitting of the t_{2g} manifold. However, the electronic situation in $RbOs_2O_6$ is expected to be quite different from $Cd_2(Os,Re)_2O_7$: The 16d site is unoccupied and the Rb^+ cation is at the 8b site. Therefore, more detailed comparisons require band-structure calculations specific for $RbOs_2O_6$.

Polycrystalline samples of $RbOs_2O_6$ have been synthesized by a procedure described in Ref. [6]. A stoichiometric amount of OsO_2 (Alfa Aesar, $99.99\,\%$) and Rb_2O (Aldrich, $99\,\%$) was thoroughly mixed in an argon dry box and pressed into a pellet. The pellet was put into a quartz tube which was evacuated and sealed. This tube was heated up to $600\,°C$ and kept at this temperature for $24\,h$. According to the X-ray diffraction analysis, the resulting sample contained 2 phases: pyrochlore $RbOs_2O_6$ and $RbOsO_4$. $RbOsO_4$ can be removed by a $2\,h$ treatment in a $10\,\%$ solution of HCl and subsequent washing in water and drying at $100\,°C$. The X-ray diffraction pattern of the purified sample is shown in Fig. 1, where all reflections can be indexed on the basis of a pyrochlore unit cell. The lattice parameter $a = 10.1137(1)\,Å$ is slightly larger than in KOs_2O_6 ($a = 10.099(1)\,Å$ [6]). The preliminary X-ray diffraction study reveals that the Rb cations occupy the 8b site in the pyrochlore lattice, as is the case for potassium in KOs_2O_6 [6]. The experimental details of the synthesis and purification of $RbOs_2O_6$ are described elsewhere [9]. KOs_2O_6 and $RbOs_2O_6$ are the only reported osmium compounds in the form AB_2O_6 [6], and both show bulk superconductivity.

The magnetic susceptibility at low temperatures, depicted in the inset of Fig. 4, shows

3

the diamagnetic transition into a bulk superconducting state. The measurements have been performed at $H = 3.3\,\text{Oe}$ in zero-field-cooled and field-cooled states.

Specific heat was measured in a physical properties measurement apparatus using an adiabatic relaxation technique (Quantum Design, PPMS). The sample was pressed into a cylindrical pellet of about $20\,\text{mg}$. The applied magnetic field was perpendicular to the cylinder axis. Figure 2 shows the specific heat C_p/T vs. T^2 for magnetic fields from 0 to $4\,\text{T}$ in $0.5\,\text{T}$ steps and also a normal state curve measured at $12\,\text{T}$.

From the normal-state curve at $12\,\text{T}$, we extract the electronic specific heat coefficient $\gamma = \lim_{T \to 0\,\text{K}} C_\text{p}/T$ by fitting the data below $4\,\text{K}$ to $C_\text{p}/T = \gamma + \beta T^n$. From this fit we get $\gamma = (33.7 \pm 0.2)\,\text{mJ/mol}_\text{f.u.}/\text{K}^2$, $\beta = (1.42 \pm 0.1)\,\text{mJ/mol}_\text{f.u.}/\text{K}^{2+\text{n}}$, and $n = 1.92 \pm 0.05$. To our knowledge, this value of γ is the largest reported for a pyrochlore compound, and we expect it to play a crucial role in the tendency for $RbOs_2O_6$ to superconduct. Since the fit to the low-temperature data yields $n < 2$, the Debye temperature $\Theta_\text{D}(T)$ in this range is slightly temperature dependent, with a value of $\Theta_\text{D}(1\,\text{K}) \approx 230\,\text{K}$ and $\Theta_\text{D}(4\,\text{K}) \approx 240\,\text{K}$. The temperature dependence of $\Theta_\text{D}(T)$ on a larger scale is typical for cubic metals [10], showing a broad minimum at about $11.5\,\text{K}$ with a value of $\Theta_\text{D}(11.5\,\text{K}) \approx 190\,\text{K}$. Towards higher temperatures Θ_D rises again to reach about $225\,\text{K}$ at $25\,\text{K}$. Compared to other metallic pyrochlores, which have a Debye temperature of typically 300 to $400\,\text{K}$, Θ_D in $RbOs_2O_6$ is rather low, indicative of lower frequency phonon modes.

In the superconducting state, a noticeable electronic density of states at the Fermi level remains as $T \to 0\,\text{K}$ (Fig. 2). This might be interpreted as a sign of an unconventional superconducting state with part of the Fermi surface ungapped. Alternatively, if part of the sample does not undergo a superconducting transition, then the measured curve is the sum of the superconducting and normal contributions. Indeed, such an analysis appears to yield consistent results, suggesting a conventional BCS-like superconducting state. Following the second interpretation, we proceed to further analyze C_p below T_c. Starting with the $12\,\text{T}$ data as the normal state reference, we subtract $23.4\,\%$ of it (shown in the inset of Fig. 2) from the $0\,\text{T}$ set. Correspondingly, the superconducting volume fraction is about $77\,\%$, similar to the estimated fraction in KOs_2O_6 [6]. The resulting specific heat for the superconducting part is shown in Fig. 3 on a semilogarithmic scale vs. T_c/T. The line indicates the expected behavior from BCS assuming an isotropic gap [11]: For $2.5 < T_\text{c}/T < 6$, the specific heat approximately follows an exponential behavior $8.5\,\gamma\,T_\text{c}\exp(-1.44\,T_\text{c}/T)$. Down to $1\,\text{K}$, the

specific heat in the superconducting state decreases in close quantitative agreement with conventional superconducting behavior. Below that, the subtraction of the two components provides unreliable results, since the difference becomes exceedingly small. Furthermore, impurities play an essential role at such low temperatures, and it is thus difficult to draw conclusions from the observed deviation. It will be worthwhile to elucidate the microscopic origin of the roughly 20% ungapped fraction, which is observed both in $RbOs_2O_6$ and KOs_2O_6 [6].

Additional support for the assumed two-component analysis comes from the specific heat anomaly at T_c: $\Delta C_p/T_c$ is estimated to $35.6\,\mathrm{mJ/mol_{f.u.}/K^2}$ (inset of Fig. 2), resulting in a normalized ratio $\Delta C_p/(76.6\%\gamma T_c) = 1.38$. The 76.6% in the denominator is the correction to ΔC_p due to the deviation of the superconducting volume fraction from 100%. This normalized specific heat jump at T_c is indeed close to the weak-coupling BCS value of 1.43. Therefore, an analysis in terms of an about 77% superconducting fraction appears reasonable, even as it implies a very similar γ for the superconducting and non-superconducting parts of the sample. Since the X-ray diffractogram (Fig. 1) shows the presence of only one phase, the structure of the non-superconducting part has to be the same as that of the superconducting one. Again, further analysis is necessary to elucidate the microscopic origin of the ungapped fraction.

Figure 4 shows the upper critical field H_{c2} extracted from specific heat measurements. T_c has been chosen such that the entropy is balanced above and below T_c from C_p/T vs. T data. The upper critical field of $RbOs_2O_6$ lies below the Pauli-limiting field $H_{p0} = 1.84\,\mathrm{T/K} \times T_c = 11.7\,\mathrm{T}$ [12]. This is in sharp contrast to KOs_2O_6, where the critical field seems to exceed the Pauli limit [6]. A power law fit $H_{c2}(T) = H_{c2}(0)(1 - (T/T_c)^n)$ (dashed line) gives an exponent of $n = 1.0 \pm 0.1$ and a critical temperature $T_c = (6.37 \pm 0.03)\,\mathrm{K}$. Such a linear behavior of H_{c2} is also observed in $Cd_2Re_2O_7$ [4, 5]. The initial slope of the critical boundary at T_c is $-\mathrm{d}(\mu_0 H_{c2})/\mathrm{d}T|_{T=T_c} = 1.2\,\mathrm{T/K}$.

The upper critical field of a superconductor is determined by the combined effect of an external magnetic field on the spin and orbital degrees of freedom of the conduction electrons. Werthamer et al. have worked out a theory for H_{c2} which includes both spin and orbital paramagnetic effects as well as nonmagnetic and spin-orbit scattering [13]. In $RbOs_2O_6$, the upper critical field does not, however, behave as predicted by the Werthamer-Helfand-Hohenberg (WHH) formula in the dirty limit, as can be seen in Fig 4. The initial

slope of the critical boundary at T_c results in a Maki-parameter $\alpha = -0.52758\,\mathrm{K/T} \times \mathrm{d}(\mu_0 H_{c2})/\mathrm{d}T|_{T=T_c} = 0.64 \pm 0.1$ [13, 14]. Spin contributions to the energy balance of a superconductor become important when $\alpha \gtrsim 1$. Applying the WHH model, we would therefore have to conclude that $\mathrm{RbOs_2O_6}$ is in the orbital limit away from the Pauli-limiting regime with an orbital critical field of $H_{c2}^*(T=0) = \alpha H_{p0}/\sqrt{2} = 5.3\,\mathrm{T}$. This field might be a good extrapolation of the critical field to $0\,\mathrm{K}$ judging from Fig. 4. However, calculations based on a realistic Fermi surface are needed to further clarify the detailed behavior of H_{c2}. Using a reasonably extrapolated H_{c2} of $6\,\mathrm{T}$, we calculate the Ginzburg-Landau coherence length at $0\,\mathrm{K}$ of $\xi = \sqrt{\Phi_0/(2\pi H_{c2})} \approx 74\,\text{Å}$, where Φ_0 is the magnetic flux quantum.

We have studied the basic thermodynamic properties of the new pyrochlore superconductor $\mathrm{RbOs_2O_6}$ with a critical temperature of $6.4\,\mathrm{K}$. The electronic density of states at the Fermi level in the normal state results in $\gamma = (33.7 \pm 0.2)\,\mathrm{mJ/mol_{f.u.}/K^2}$, the highest reported value for a pyrochlore. Together with the high γ, we expect the large Os - O - Os angle of $139.4\,^\circ$ to play a crucial role in the tendency towards superconductivity. The inherent geometrical frustration of the three dimensional tetrahedral Os sublattice attributes further importance to this new superconductor. We find that a careful analysis of the specific heat data, taking into account the normal-state volume fraction, implies conventional BCS-type behavior. Although the compound could be expected to be only marginally different from the related compound $\mathrm{KOs_2O_6}$, a significant difference in the magnitude of the upper critical field H_{c2} is observed. Considering the potential for competing electronic groundstates in these compounds, the pyrochlore type superconductors may be of fundamental importance to address unsolved issues.

---

[1] A. P. Ramirez, Annu. Rev. Mater. Sci. **24**, 453 (1994).

[2] M. A. Subramanian, G. Aravamudan, and G. V. S. Rao, Prog. Solid St. Chem. **15**, 55 (1983).

[3] M. Hanawa, Y. Muraoka, T. Tayama, T. Sakakibara, J. Yamaura, and Z. Hiroi, Phys. Rev. Lett. **87**, 187001 (2001).

[4] H. Sakai, K. Yoshimura, H. Ohno, H. Kato, S. Kambe, R. E. Walstedt, T. D. Matsuda, Y. Haga, and Y. Onuki, J. Phys.: Condens. Matter **13**, L785 (2001).

[5] R. Jin, J. He, S. McCall, C. S. Alexander, F. Drymiotis, and D. Mandrus, Phys. Rev. B **64**, 180503 (2001).

[6] S. Yonezawa, Y. Muraoka, Y. Matsushita, and Z. Hiroi, J. Phys.: Condens. Matter **16**, L9 (2004).

[7] Z. Hiroi, S. Yonezawa, and Y. Muraoka, cond-mat/0402006.

[8] D. J. Singh, P. Blaha, K. Schwarz, and J. O. Sofo, Phys. Rev. B **65**, 155109 (2002).

[9] S. M. Kazakov, N. D. Zhigadlo, M. Brühwiler, B. Batlogg, and J. Karpinski, to be published.

[10] D. H. Parkinson, Rep. Prog. Phys. **21**, 226 (1958).

[11] J. Bardeen and J. R. Schrieffer, *Recent Developments in Superconductivity*, vol. III of *Progress in low temperature physics* (north-holland, 1961).

[12] A. M. Clogston, Phys. Rev. Lett. **9**, 266 (1962).

[13] N. R. Werthamer, E. Helfand, and P. C. Hohenberg, Phys. Rev. **147**, 295 (1966).

[14] K. Maki, Physics **1**, 127 (1964).

FIG. 1: The powder X-ray diffraction pattern of the purified sample, where all reflections can be indexed on the basis of a pyrochlore face-centered unit cell with lattice parameter $a = 10.1137(1)\,\text{Å}$. The inset shows an Os atom and its relationship to its surrounding. Every Os atom forms the shared corner of two Os tetrahedra in a network. The exchange pathways to the nearest neighbors, leading by one of the coordinating oxygen atoms, are shown by dashed lines. The Rb cations are omited in this illustration for clarity.
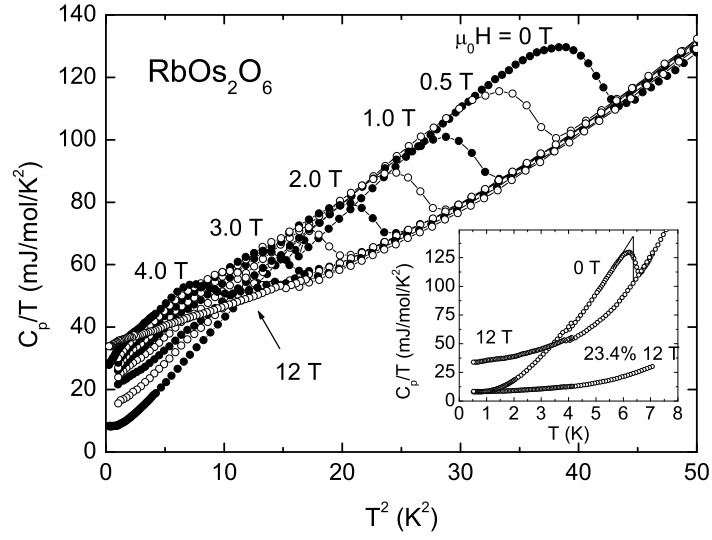

FIG. 2: Specific heat C_p/T vs. T^2 for magnetic fields from 0 to 4 T in 0.5 T steps and 12 T. From the normal-state curve at 12 T, we extract the electronic specific heat coefficient $\gamma = \lim_{T \to 0\,\text{K}} C_p/T = (33.7 \pm 0.2)\,\text{mJ/mol}_{\text{f.u.}}/\text{K}^2$. The Debye temperature $\Theta_D(T)$ below 4 K is slightly temperature dependent, with a value of $\Theta_D(1\,\text{K}) \approx 230\,\text{K}$ and $\Theta_D(4\,\text{K}) \approx 240\,\text{K}$. The inset shows the 0 T and normal state specific heat on a linear T scale. Also shown is 23.4 % of the normal state C_p, expected to be present in the superconducting C_p, and used for our analysis. The normalized specific heat jump at T_c, $\Delta C_p/(76.6\,\%\gamma T_c) = 1.38$, is close to the weak-coupling BCS value of 1.43.
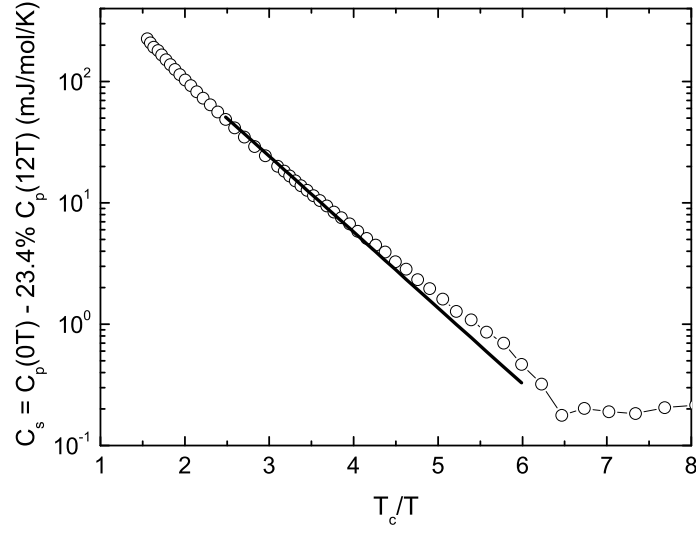
FIG. 3: Superconducting specific heat calculated by subtracting 23.4% of the normal state specific heat at $12\,\mathrm{T}$, plotted on a semilogarithmic scale vs. T_c/T. The corresponding superconducting volume fraction is thus about 77%, similar to the estimated fraction in $\mathrm{KOs_2O_6}$ [6]. The line indicates the expected behavior from BCS assuming an isotropic gap: For $2.5 < T_\mathrm{c}/T < 6$, the specific heat approximately follows an exponential behavior $8.5\,\gamma\,T_\mathrm{c}\exp(-1.44\,T_\mathrm{c}/T)$. Down to $1\,\mathrm{K}$, the superconducting specific heat decreases in close quantitative agreement with this conventional superconducting behavior.
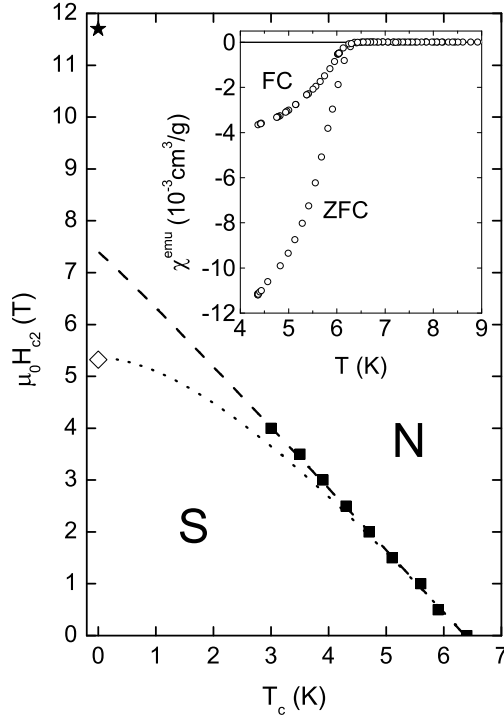
FIG. 4: Upper critical field H_{c2} extracted from specific heat measurements. A power law fit $H_{c2}(T) = H_{c2}(0)(1 - (T/T_c)^n)$ (dashed line) gives an exponent of $n = 1.0 \pm 0.1$ and a critical temperature $T_c = (6.37 \pm 0.03)\,\text{K}$. The initial slope of the critical boundary at T_c is $-\mathrm{d}(\mu_0 H_{c2})/\mathrm{d}T|_{T=T_c} = 1.2\,\text{T/K}$. The dotted line is a fit to the WHH formula in the orbital limit ($\lambda_{\text{SO}} = \infty$) using the calculated Maki parameter $\alpha = 0.64$. Also shown are the Pauli limiting field H_{p0} ($\star$) and the orbital limiting field H_{c2}^* ($\diamond$). The magnetic susceptibility at low temperatures, depicted in the inset, shows the diamagnetic transition into a bulk superconducting state. The magnetization measurements have been performed at $H = 3.3\,\text{Oe}$ in zero-field-cooled (ZFC) and field-cooled (FC) states.

This figure "XRDGraph.png" is available in "png" format from:

http://arXiv.org/ps/cond-mat/0403526v1